Exact solution of the one-dimensional anisotropic t - J model: ground-state properties and the excitation spectrum

1996 J. Phys.: Condens. Matter 8 8363

(http://iopscience.iop.org/0953-8984/8/43/027)

J. Phys.: Condens. Matter **8** (1996) 8363–8378. Printed in the UK

Exact solution of the one-dimensional anisotropic *t–J* model: ground-state properties and the excitation spectrum

R Sato†

Department of Physics, Faculty of Science, Osaka University, Toyonaka, Osaka 560, Japan

Received 2 April 1996, in final form 16 July 1996

Abstract. The one-dimensional anisotropic t–J model was exactly solved using the Bethe *ansatz*. We first discuss the effect of anisotropy on the ground-state properties. We find a continuous phase transition induced by a magnetic field. The low-lying (spin and charge) excitation spectrum is obtained for various fillings. According to the anisotropy, the model has massive or massless modes for spin excitations. At half-filling, the model reduces to the spin-$\frac{1}{2}$ antiferromagnetic *XXZ*-model. We calculate the correct excitation continuum whose lowest mode is lower than that obtained by des Cloizeaux and Gaudin. Charge excitations are massless for any value of the anisotropy.

1. Introduction

In recent years the t–J model [1, 2] has been intensively studied as a candidate for a model for high-T_c superconductivity. It is argued [3] that strongly correlated electronic systems in one and two dimensions may share common aspects, so it is crucial to obtain exact results in one dimension. The one-dimensional (1D) isotropic t–J model at its 'supersymmetric' point is exactly solvable using the (nested) Bethe *ansatz* [4, 5] and various properties of the model have been studied by many authors [6–11]. Even more recently, several versions of the solvable anisotropic t–J model with certain quantum group symmetries have been considered [12–17]. One characteristic property of the anisotropic t–J model is that the superconducting correlation dominates other correlations [14, 16]. This property is not present for the usual (isotropic) supersymmetric t–J model [9] (see also [18]). In this paper we will study the 1D anisotropic supersymmetric t–J model which is exactly solvable using the Bethe *ansatz*. In particular, we discuss the ground-state properties in relation to anisotropy and magnetic field, and also obtain the low-lying (spin and charge) excitation spectrum.

We consider the anisotropic t–J model with $\mathrm{spl}_q(2,1)$ supersymmetry on a 1D lattice of L sites, which is defined by the Hamiltonian ($\langle i, j\rangle$ denotes neighbouring sites)

$$\mathcal{H}^{(0)} = \mathcal{P}\Bigg\{-t\sum_{\langle i,j\rangle,\sigma}(c^\dagger_{i\sigma}c_{j\sigma} + \mathrm{HC}) + \frac{J}{2}\sum_{\langle i,j\rangle,\sigma} c^\dagger_{i\sigma}c_{i-\sigma}c^\dagger_{j-\sigma}c_{j\sigma} - \frac{J}{2}\sum_i(q^{-1}n_{i\downarrow}n_{i+1\uparrow} + qn_{i\uparrow}n_{i+1\downarrow})\Bigg\}\mathcal{P} \qquad (1)$$

† E-mail: satow@godzilla.phys.sci.osaka-u.ac.jp.

0953-8984/96/438363+16$19.50

or, in a more transparent form,

$$\mathcal{H}^{(0)} = \mathcal{P}\Biggl\{-t\sum_{\langle i,j\rangle,\sigma}(c^\dagger_{i\sigma}c_{j\sigma}+\mathrm{HC}) - \frac{q-q^{-1}}{2}J\sum_{\langle i,j\rangle}\frac{1}{2}(n_iS^z_j - S^z_in_j) + J\sum_{\langle i,j\rangle}\biggl[S^x_iS^x_j + S^y_iS^y_j + \frac{q+q^{-1}}{2}\biggl(S^z_iS^z_j - \frac{1}{4}n_in_j\biggr)\biggr]\Biggr\}\mathcal{P} + \frac{q+q^{-1}}{2}J\sum_i n_i. \tag{2}$$

Here $c^\dagger_{j\sigma}$ ($c_{j\sigma}$) is the creation (annihilation) operator for electrons ($\sigma = \uparrow, \downarrow$), and $n_j = n_{j\uparrow} + n_{j\downarrow}$ ($n_{j\sigma} = c^\dagger_{j\sigma}c_{j\sigma}$) denotes the number operator. The projector $\mathcal{P}$ restricts the Hilbert space to that of no double occupancy. One should note that the Hamiltonian $\mathcal{H}^{(0)}$ explicitly breaks the time-reversal symmetry. The parameter q determines the anisotropy of the model. At half-filling the model reduces to the spin-$\frac{1}{2}$ *XXZ*-model (up to an irrelevant constant term). We shall consider the model in a magnetic field h and with a chemical potential μ:

$$\mathcal{H} = \mathcal{H}^{(0)} - \frac{h}{2}\sum_i(n_{i\uparrow} - n_{i\downarrow}) + \mu\sum_i n_i. \tag{3}$$

In the isotropic limit $q \to 1$, the Hamiltonian $\mathcal{H}$ with $\mu = -J$ reduces to the usual (isotropic) t–J model [8]. The anisotropic t–J model is exactly solvable when $J = \pm 2t$. It is convenient to parametrize q in order to specify the region (hyperbolic or trigonometric) of anisotropy of the model as follows:

$$\Delta \equiv \frac{q+q^{-1}}{2} = \begin{cases}\cosh\gamma & (q = \mathrm{e}^{\gamma},\ \Delta > 1)\\ \cos\gamma & (q = \mathrm{e}^{\mathrm{i}\gamma},\ |\Delta| \leqslant 1).\end{cases} \tag{4}$$

In the trigonometric region, the Hamiltonian $\mathcal{H}^{(0)}$ (and also $\mathcal{H}$) is not hermitian; however, it possesses real eigenvalues [12]. In what follows we concentrate on the region where $\Delta \geqslant 0$ which is of physical relevance. We also set $t = 1$ and $J = 2$, i.e., we treat the model with ‘antiferromagnetic’ interaction.

2. Ground-state properties

In this section we discuss the ground-state properties of the anisotropic t–J model (3) with $J = 2t$ in relation to the anisotropy and magnetic field. The model can be diagonalized using the Bethe *ansatz* [19–21]. As is the case for the usual supersymmetric t–J model [10], we have three possible types of Bethe *ansatz* equation, depending on what kind of ‘grading’ we choose. It is convenient to employ the so-called Sutherland representation [5] (where we regard the state with all of the sites occupied by up-spin electrons as the background (reference state)), since no complex roots of the Bethe *ansatz* equations are present in the ground states and low-lying excited states at zero temperature.

The Bethe *ansatz* equations with periodic boundary conditions in the Sutherland representation take the form (for L even)

$$\left[\frac{F(\lambda_j - \mathrm{i}\gamma/2)}{F(\lambda_j + \mathrm{i}\gamma/2)}\right]^L = -\prod_{\alpha=1}^{N_h}\frac{F(\lambda_j - \Lambda_\alpha + \mathrm{i}\gamma/2)}{F(\lambda_j - \Lambda_\alpha - \mathrm{i}\gamma/2)}\prod_{k=1}^{M}\frac{F(\lambda_j - \lambda_k - \mathrm{i}\gamma)}{F(\lambda_j - \lambda_k + \mathrm{i}\gamma)} \qquad 1 \leqslant j \leqslant M \tag{5}$$

$$\prod_{k=1}^{M}\frac{F(\Lambda_\alpha - \lambda_k - \mathrm{i}\gamma/2)}{F(\Lambda_\alpha - \lambda_k + \mathrm{i}\gamma/2)} = 1 \qquad 1 \leqslant \alpha \leqslant N_h \tag{6}$$

where $N_\uparrow$ ($N_\downarrow$) is the number of up-spin (down-spin) electrons, N_h is the number of empty sites, and $M = N_\downarrow + N_h$. The number of electrons is denoted by N_e $(= N_\uparrow + N_\downarrow)$. The function $F(\alpha)$ is defined by

$$F(\alpha) := \begin{cases} \sinh\alpha & (\Delta > 1) \\ \sin\alpha & (0 \leqslant \Delta < 1). \end{cases} \tag{7}$$

The total energy and momentum are written in terms of the solutions of (5) and (6) as

$$E = 2f(\gamma)L - \sum_{j=1}^{M} g(\lambda_j) - \frac{h}{2}(N_\uparrow - N_\downarrow) + \mu N_e \tag{8}$$

$$P = (L-1)\pi - \mathrm{i}\sum_{j=1}^{M} \ln\left(\frac{F(\lambda_j - \mathrm{i}\gamma/2)}{F(\lambda_j + \mathrm{i}\gamma/2)}\right) \tag{9}$$

where the functions $f(\alpha)$ and $g(\alpha)$ are respectively defined by

$$f(\gamma) := \begin{cases} \cosh\gamma & (\Delta > 1) \\ \cos\gamma & (0 \leqslant \Delta < 1). \end{cases} \tag{10}$$

$$g(\alpha) := \begin{cases} \dfrac{2\sinh^2\gamma}{\cosh\gamma - \cos 2\alpha} & (\Delta > 1) \\ \dfrac{2\sin^2\gamma}{\cosh 2\alpha - \cos\gamma} & (0 \leqslant \Delta < 1). \end{cases} \tag{11}$$

Taking the logarithm of the equations (5) and (6), we arrive at

$$L\theta(2\lambda_j) = 2\pi I_j - \sum_{\alpha=1}^{N_h} \theta(2(\lambda_j - \Lambda_\alpha)) + \sum_{k=1}^{M} \theta(\lambda_j - \lambda_k) \tag{12}$$

$$\sum_{k=1}^{M} \theta(2(\Lambda_\alpha - \lambda_k)) = 2\pi J_\alpha \tag{13}$$

where $\theta(\alpha) = 2\arctan[\coth(\gamma/2)\tanh\alpha]$. The integers or half odd integers I_j and J_α characterize the eigenstates. In the thermodynamic limit, the continuous densities $\rho_s^{(0)}(\lambda)$ and $\rho_c^{(0)}(\Lambda)$ of the distributions of the (spin and charge) rapidities for the ground state are obtained as the solutions of the following set of coupled integral equations (superscript '(0)' indicates the ground state):

$$\begin{aligned} \rho_s^{(0)}(\lambda) &= S_2(\lambda) + \int_{-Q}^{Q} \mathrm{d}\lambda'\ S_1(\lambda - \lambda')\rho_s^{(0)}(\lambda) + \int_{-B}^{B} \mathrm{d}\Lambda'\ S_2(\lambda - \Lambda')\rho_c^{(0)}(\Lambda') \\ \rho_c^{(0)}(\Lambda) &= \int_{-Q}^{Q} \mathrm{d}\lambda'\ S_2(\Lambda - \lambda')\rho_s^{(0)}(\lambda') \end{aligned} \tag{14}$$

with

$$S_1(\alpha) = -\phi(\alpha, 2\gamma) \qquad S_2(\alpha) = \phi(\alpha, \gamma) \tag{15}$$

where the function $\phi(\alpha, \gamma)$ is defined by

$$\phi(\alpha, \gamma) := \begin{cases} \dfrac{1}{\pi}\dfrac{\sinh\gamma}{\cosh\gamma - \cos 2\alpha} & (\Delta > 1) \\ \dfrac{1}{\pi}\dfrac{\sin\gamma}{\cosh 2\alpha - \cos\gamma} & (0 \leqslant \Delta < 1). \end{cases} \tag{16}$$

The integration limits Q and B determine the densities ($0 \leqslant Q, B \leqslant \pi/2$ for $\Delta > 1$ and $0 \leqslant Q, B \leqslant \infty$ for $0 \leqslant \Delta < 1$):

$$\int_{-Q}^{Q} \mathrm{d}\lambda\ \rho_s^{(0)}(\lambda) = M/L = (N_\downarrow + N_h)/L = m = n_\downarrow + n_h \tag{17}$$

$$\int_{-B}^{B} \mathrm{d}\Lambda\ \rho_c^{(0)}(\Lambda) = N_h/L = (L - N_e)/L = n_h = 1 - n_e. \tag{18}$$

The magnetization and the ground-state energy are given by

$$\sigma = S^z_{total}/L = \frac{1}{2} - \int_{-Q}^{Q} \mathrm{d}\lambda\ \rho_s^{(0)}(\lambda) + \frac{1}{2}\int_{-B}^{B} \mathrm{d}\Lambda\ \rho_c^{(0)}(\Lambda) \tag{19}$$

$$e = E/L = 2f(\gamma) - \int_{-Q}^{Q} \mathrm{d}\lambda\ g(\lambda)\rho_s^{(0)}(\lambda) - h\sigma + \mu n_e. \tag{20}$$

Note that at half-filling these Bethe *ansatz* equations reduce to those for the spin-$\frac{1}{2}$ *XXZ*-chain [22]:

$$H = \frac{1}{2}\sum_{i=1}^{L} (\sigma_i^x \sigma_{i+1}^x + \sigma_i^y \sigma_{i+1}^y + \Delta \sigma_i^z \sigma_{i+1}^z) \tag{21}$$

($\{\sigma^a\}$ $(a = x, y, z)$ are the Pauli matrices) with the same value of Δ (or γ).

To express several physical quantities as implicit functions of Q and B, we employ the 'dressed-charge-matrix' formalism [23, 24]. We first rewrite the equations (14) as a matrix integral equation of the form

$$\rho^{(0)}(\lambda, \Lambda) = \rho_0^{(0)}(\lambda, \Lambda) + K(\lambda, \Lambda; \lambda', \Lambda')\rho^{(0)}(\lambda', \Lambda') \tag{22}$$

with

$$\rho^{(0)}(\lambda, \Lambda) \equiv \begin{pmatrix} \rho_s^{(0)}(\lambda) \\ \rho_c^{(0)}(\Lambda) \end{pmatrix} \qquad \rho_0^{(0)}(\lambda, \Lambda) = \begin{pmatrix} S_2(\lambda) \\ 0 \end{pmatrix}. \tag{23}$$

The integral-kernel matrix K is defined by

$$K(\lambda, \Lambda; \lambda', \Lambda') \equiv \begin{pmatrix} K_{11}(\lambda - \lambda') & K_{12}(\lambda - \Lambda') \\ K_{21}(\Lambda - \lambda') & K_{22}(\Lambda - \Lambda') \end{pmatrix} = \begin{pmatrix} S_1(\lambda - \lambda') & S_2(\lambda - \Lambda') \\ S_2(\Lambda - \lambda') & 0 \end{pmatrix} \tag{24}$$

whose elements operate on a scalar function $A(x)$ as

$$K_{\alpha\beta}(\lambda - \lambda')A(\lambda') = \int_{-a_\beta}^{a_\beta} \mathrm{d}\lambda'\ K_{\alpha\beta}(\lambda - \lambda')A(\lambda') \qquad a_1 = Q \qquad a_2 = B. \tag{25}$$

The dressed charge matrix $\Xi(\lambda, \Lambda)$ and the dressed energy (in zero magnetic field) $\varepsilon(\lambda, \Lambda)$ [23, 24],

$$\Xi(\lambda, \Lambda) \equiv \begin{pmatrix} \xi_{11}(\lambda) & \xi_{12}(\Lambda) \\ \xi_{21}(\lambda) & \xi_{22}(\Lambda) \end{pmatrix} \qquad \varepsilon(\lambda, \Lambda) \equiv \begin{pmatrix} \varepsilon_1(\lambda) \\ \varepsilon_2(\Lambda) \end{pmatrix} \tag{26}$$

also obey equations similar to (22) with the respective inhomogeneous terms

$$\Xi_0(\lambda, \Lambda) = \begin{pmatrix} 1 & 0 \\ 0 & 1 \end{pmatrix} \qquad \varepsilon_0(\lambda, \Lambda) \equiv \begin{pmatrix} \varepsilon_{01}(\lambda) \\ \varepsilon_{02}(\Lambda) \end{pmatrix} = \begin{pmatrix} -g(\lambda) \\ 0 \end{pmatrix}. \tag{27}$$

In the spirit of Woynarovich and Penc [25], we can derive the expressions for the magnetic field h, the chemical potential μ, and the magnetic susceptibility χ as functions of Q and B (for a detailed account of the formalism, see [25, 26, 11]). The results are

$$h(Q,B) = \frac{-\varepsilon_1(Q)\xi_{22}(B) + \varepsilon_2(B)\xi_{12}(Q)}{\det \Xi(Q,B)} \tag{28}$$

$$\mu(Q,B) = \frac{\varepsilon_1(Q)[2\xi_{21}(B) - \xi_{22}(B)] - \varepsilon_2(B)[2\xi_{11}(Q) - \xi_{12}(Q)]}{2\det \Xi(Q,B)} \tag{29}$$

$$\chi^{-1}(Q,B) = \frac{v_1(Q)(\xi_{22}(B))^2 + v_2(B)(\xi_{12}(Q))^2}{2\det \Xi(Q,B)}. \tag{30}$$

The factors $v_1(Q)$ and $v_2(B)$ in (30) are the Fermi velocities (times 2π) [24].

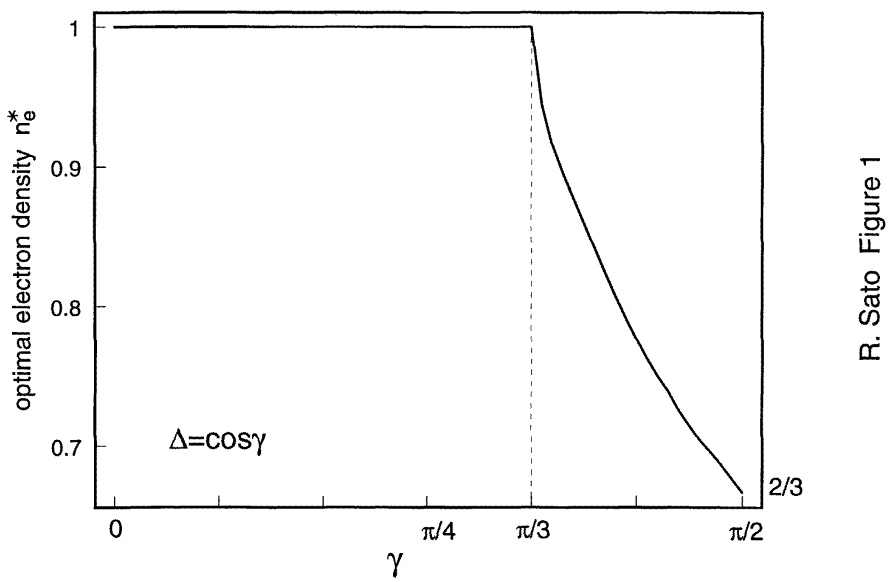

Figure 1. The optimal (ground-state) electron density n_e^* as a function of the anisotropy γ in the grand canonical ensemble with $\mu = -2f(\gamma) = -2\cos\gamma$ (in the trigonometric region, $\Delta = \cos\gamma$). $n_e^* = \frac{2}{3}$ for $\gamma = \frac{1}{2}\pi$ ($\Delta = 0$).

In what follows in this section, we will consider the model in the grand canonical ensemble for convenience. We first investigate the effect of anisotropy on the ground state in zero magnetic field ($Q = \pi/2$, or ∞). From (14)–(20) we can determine the optimal electron density n_e^* for which the model has the lowest energy among all fillings when a value of the anisotropy γ is given. Here we set $\mu = -2f(\gamma)$ for comparison with the isotropic case. We obtained that

$$\begin{aligned} n_e^* &= 1 \qquad \text{for } \Delta \geqslant \tfrac{1}{2} \\ n_e^* &\neq 1 \qquad \text{for } \Delta < \tfrac{1}{2}. \end{aligned} \tag{31}$$

(see figure 1). That is, for $\Delta \geqslant \frac{1}{2}$ the ground state of the anisotropic t–J model is that of the spin-$\frac{1}{2}$ *XXZ*-model with the same value of Δ (or γ). The present result includes the result for the isotropic t–J model ($\gamma = 0$) where the half-filling case gives the lowest energy among all fillings [8]. As $\Delta \to 0$ ($\gamma \to \frac{1}{2}\pi$ in the trigonometric region), the ground state approaches the symmetrical point $n_\uparrow = n_\downarrow = n_h = \frac{1}{3}$.

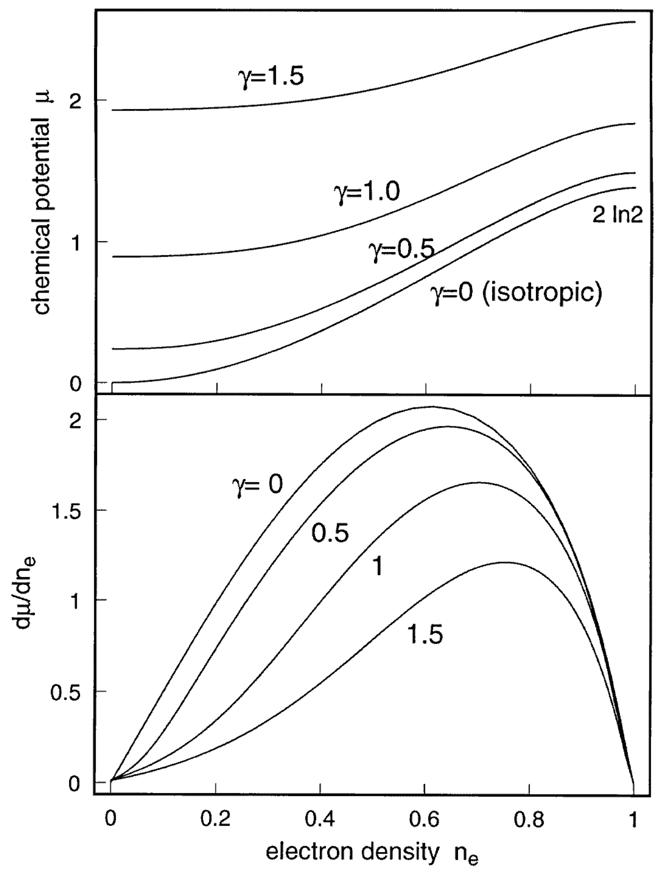

Figure 2. The chemical potential μ and its derivative versus electron density n_e for various values of the anisotropy γ in the hyperbolic region ($\Delta = \cosh\gamma$).

Both the chemical potential and its derivative with respect to the electron density n_e for different values of γ in the hyperbolic region ($\Delta = \cosh\gamma$) are shown in figure 2. We set $h = 0$ here. At half-filling ($B = 0$) we explicitly obtain

$$\mu\left(\frac{\pi}{2}, 0\right) = \sinh\gamma \left[1 + 2\sum_{m=1}^{\infty}(1 - \tanh(m\gamma))\right]. \tag{32}$$

We can perform a similar calculation in the trigonometric region ($\Delta = \cos\gamma$) and have

$$\mu(\infty, 0) = \int_{-\infty}^{\infty} \mathrm{d}\alpha \, \frac{\gamma \sin\gamma}{\cosh(\pi\alpha)(\cosh(2\gamma\alpha) - \cos\gamma)}. \tag{33}$$

The compressibility κ becomes larger as the anisotropy becomes stronger, since $\kappa^{-1} \propto \mathrm{d}\mu/\mathrm{d}n_e$. This is compatible with the fact that the region of superconductivity is larger for stronger anisotropy [16].

Consider next the magnetic property of the model. From (28) and (30) we can obtain the inverse magnetic susceptibility χ^{-1} as a function of the magnetic field h. For $\Delta \geqslant 1$ (including the isotropic t–J model), the susceptibility $\chi(h)$ as well as the magnetization curve are the same as those of the spin-$\frac{1}{2}$ XXZ-chain (the XXX-chain for $\Delta = 1$). For $\Delta < 1$,

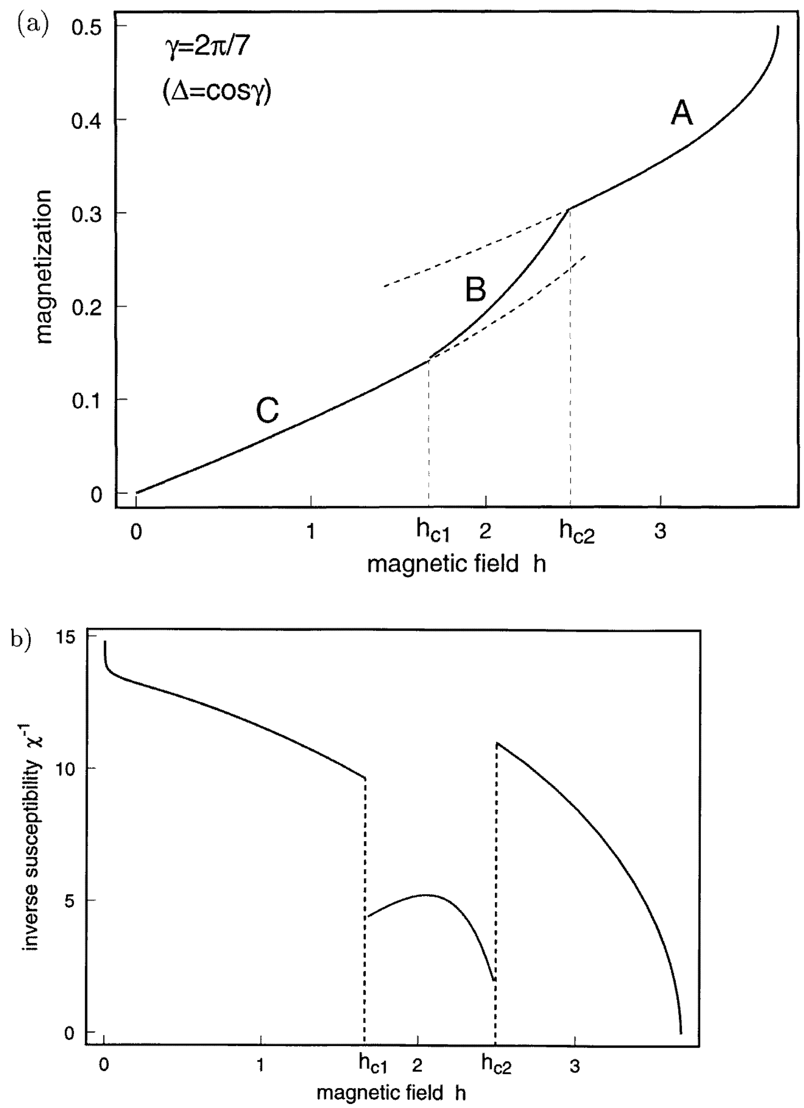

Figure 3. Magnetic properties in the grand canonical ensemble for $\Delta = \cos\gamma$ with $\gamma = 2\pi/7$. (a) The magnetization curve. Curve A is given by that for the sector with $N_\downarrow = 0$, curve B for the sector with $N_\downarrow, N_h \neq 0$ and curve C for the sector with $N_h = 0$, respectively. (b) The inverse magnetic susceptibility χ^{-1} as a function of magnetic field h. The transition points are $h_{c1} = 1.67\ldots$ and $h_{c2} = 2.46\ldots$.

on the other hand, we found a magnetic phase transition. The magnetization curve and the inverse susceptibility $\chi^{-1}(h)$ for $\Delta = \cos(2\pi/7)$ are shown as an example in figure 3. In this case, the high-field curve (curve A in figure 3) is obtained by solving the Bethe *ansatz* equations (14) with the constraint $N_\downarrow = 0$. The low-field curve (curve C) is obtained with the condition $N_h = 0$ and is the same as a part of the magnetization curve of the spin-$\frac{1}{2}$ *XXZ*-chain. For moderate values of h (curve B) we have to solve the equations under the condition $N_\downarrow, N_h \neq 0$. We have then three different phases according to the range of

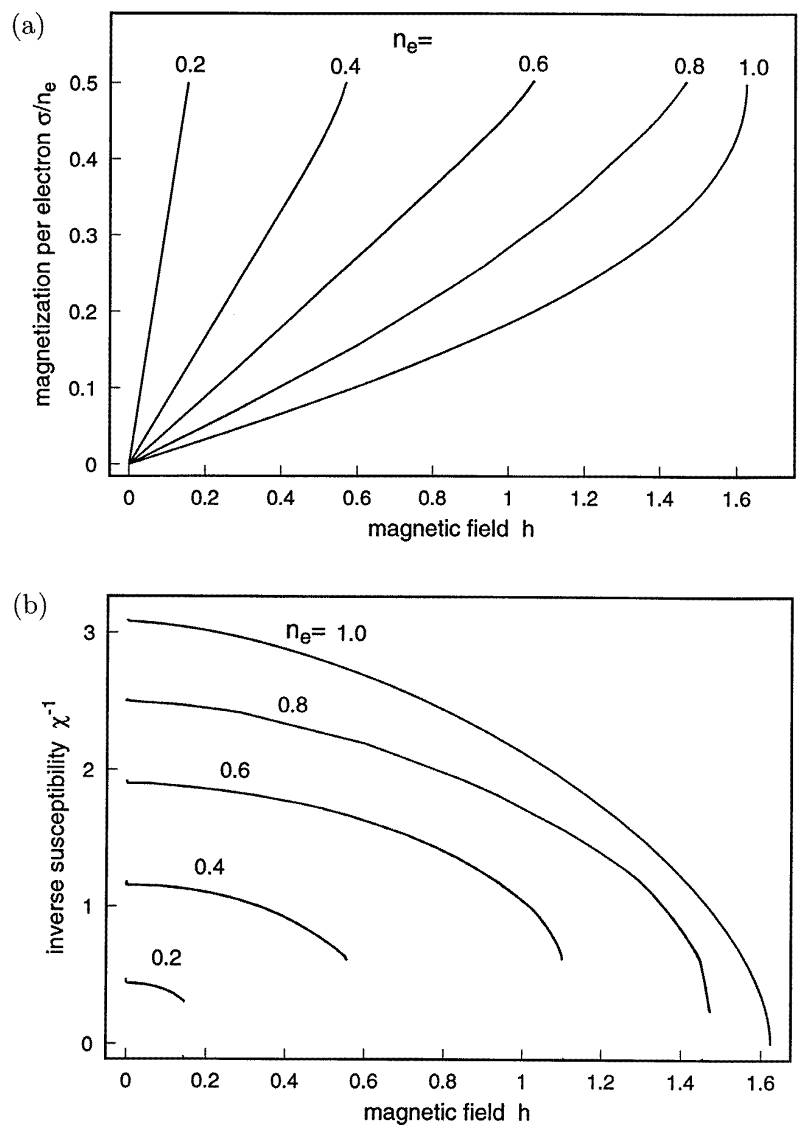

Figure 4. Magnetic properties for various fixed electron densities n_e ($\Delta = \cos\gamma$ with $\gamma = 2\pi/7$). (a) The magnetization curve σ versus h. (b) The inverse magnetic susceptibility χ^{-1} as a function of the magnetic field h.

the magnetic field. The phase transition is of second order since the magnetization curve is continuous and the magnetic susceptibility shows finite discontinuity at the transition points h_{c1} and h_{c2}. We estimate the exact values of h_{c1} and h_{c2} as $h_{c1} = 1.67\ldots$ and $h_{c2} = 2.46\ldots$. For $0 \leqslant \Delta < \frac{1}{2}$, the low-field part of the magnetization corresponding to the curve C in figure 3 disappears, so we have only one phase transition point.

To complement the above description, we show in figure 4 the magnetization curve and the magnetic susceptibility when electron densities are fixed. The saturation field h_s is explicitly given by $h_s = (1 + \Delta)\sin^2(\pi n_e/2)$. At half-filling we reproduce the results for the spin-$\frac{1}{2}$ *XXZ*-chain. The magnetic susceptibility at magnetic saturation is divergent only at half-filling.

3. The excitation spectrum

In this section we study the low-lying excitations over the ground state. Bares, Blatter and Ogata calculated the excitation spectrum of the usual (isotropic) t–J model [8]. Below we will make a similar analysis on the anisotropic t–J model. Calculations are simplified by taking the dressed-charge-matrix formalism [23, 24]. Here we are mainly interested in the hyperbolic region where $\Delta > 1$. We find a notable fact in this region (in the trigonometric region $0 \leqslant \Delta < 1$, the results are rather similar to those for the isotropic model). We calculate the excitations with the number of electrons fixed. We assume L even and $h = 0$.

3.1. Spin excitations

Spin excitations are obtained by varying the sequence $\{I_j\}$ in (12) from its ground-state configuration. Following Faddeev and Takhtajan [27], we have two types of the *physical* (spin-wave-type) excitation. One of them is constructed by having an even number $2N$ of 'holes' in the distribution of the λ-rapidities, denoted by real numbers λ_{jh} $(j = 1, 2, \ldots, 2N)$ which correspond to the holes $\{I_{jh}\}$ in the sequence $\{I_j\}$. The total spin of this excitation is $S = S^z_{total} = N$ and we have spin-multiplet excitations. In the thermodynamic limit, we obtain a set of coupled integral equations:

$$\begin{aligned}\rho_s(\lambda) &= S_2(\lambda) + \int_{-Q}^{Q} \mathrm{d}\lambda'\ S_1(\lambda - \lambda')\rho_s(\lambda) + \int_{-B}^{B} \mathrm{d}\Lambda'\ S_2(\lambda - \Lambda')\rho_c(\Lambda') \\ &\quad - \frac{1}{L}\sum_{j=1}^{2N} \delta(\lambda - \lambda_{jh}) \qquad (34)\\ \rho_c(\Lambda) &= \int_{-Q}^{Q} \mathrm{d}\lambda'\ S_2(\Lambda - \lambda')\rho_s(\lambda')\end{aligned}$$

where the functions $S_1(\alpha)$ and $S_2(\alpha)$ are given in (15). At half-filling these equations reduce to those for the spin-$\frac{1}{2}$ *XXZ*-model. We define the 'order-$1/L$' change of the continuous root densities:

$$\sigma(\lambda, \Lambda)/L = \begin{pmatrix} \sigma_1(\lambda)/L \\ \sigma_2(\lambda)/L \end{pmatrix} = \begin{pmatrix} \rho_s(\lambda) - \rho_s^{(0)}(\lambda) \\ \rho_c(\lambda) - \rho_c^{(0)}(\lambda) \end{pmatrix}.$$

From the equations (14) and (34) we can write a set of coupled integral equations for $\sigma(\lambda, \Lambda)$ as

$$\sigma(\lambda, \Lambda) = \psi(\lambda, \Lambda) + K(\lambda, \Lambda; \lambda', \Lambda')\sigma(\lambda', \Lambda') \qquad (35)$$

with

$$\psi(\lambda, \Lambda) \equiv \begin{pmatrix} \psi_1(\lambda) \\ \psi_2(\Lambda) \end{pmatrix} = \begin{pmatrix} -\sum_{j=1}^{2N} \delta(\lambda - \lambda_{jh}) \\ 0 \end{pmatrix}. \qquad (36)$$

The integral-kernel matrix K is given as (24).

The excitation energy ϵ is calculated to be

$$\epsilon = L\left\{\int_{-Q}^{Q} \mathrm{d}\lambda\ \varepsilon_{01}(\lambda)(\rho_s(\lambda) - \rho_s^{(0)}(\lambda)) + \int_{-B}^{B} \mathrm{d}\Lambda\ \varepsilon_{02}(\Lambda)(\rho_c(\Lambda) - \rho_c^{(0)}(\Lambda))\right\}$$

$$= \sum_{\alpha=1}^{2}\int_{-a_\alpha}^{a_\alpha}\mathrm{d}\mu_\alpha\ \varepsilon_{0\alpha}(\mu_\alpha)\sigma_\alpha(\mu_\alpha) = \sum_{\alpha=1}^{2}\int_{-a_\alpha}^{a_\alpha}\mathrm{d}\mu_\alpha\ \varepsilon_\alpha(\mu_\alpha)\Psi_\alpha$$
$$= -\sum_{i=1}^{2N}\varepsilon_1(\lambda_{ih}). \tag{37}$$

The momentum of the excitation (measured from the ground state) is given by

$$p = \frac{\pi}{L}(L \pm \nu N_h^{(0)}) - \frac{2\pi}{L}\sum_{i=1}^{2N} I_{ih} = \pm\nu k_F - \frac{2\pi}{L}\sum_{i=1}^{2N} I_{ih}$$
$$= \pm\,\nu k_F - 2\pi\sum_{j=1}^{2N}\int_0^{\lambda_{jh}}\mathrm{d}\lambda\ \rho_s^{(0)}(\lambda) \qquad (\mathrm{mod}\ 2\pi) \tag{38}$$

where $\nu = 0$ for even N and $\nu = 1$ for odd N. The last equality in (38) is valid to order $1/L$. The effective Fermi momentum is defined by $k_F = \pi n_e/2$. At half-filling we reproduce the expression for the contribution from each hole, which is obtained for the spin-$\frac{1}{2}$ *XXZ*-model [28]:

$$\epsilon(\lambda) = \frac{K}{\pi}\sinh\gamma\ \mathrm{dn}\left(\frac{2K\lambda}{\pi}, k\right) \tag{39}$$
$$p(\lambda) = -\frac{\pi}{2} + \mathrm{am}\left(\frac{2K\lambda}{\pi}, k\right) \qquad -\frac{\pi}{2} \leqslant \lambda \leqslant \frac{\pi}{2} \tag{40}$$

in the hyperbolic region ($\Delta = \cosh\gamma$) and

$$\epsilon(\lambda) = \frac{\pi\sin\gamma}{\gamma\cosh(\pi\lambda/\gamma)} \tag{41}$$
$$p(\lambda) = -\frac{\pi}{2} + \arctan\left[\sinh(\pi\lambda/\gamma)\right] \qquad -\infty < \lambda < \infty \tag{42}$$

in the trigonometric region ($\Delta = \cos\gamma$), respectively. Here K is the complete elliptic integral with modulus k of $K'/K = \gamma/\pi$. Notice that $\epsilon(\pm\pi/2) > 0$ (i.e., massive) for $\gamma \neq 0$ in the hyperbolic region and $\epsilon(\pm\infty) = 0$ (i.e., massless) in the trigonometric region.

Let us consider the simplest case ($N = 1$), i.e., the spin-triplet excitation. In this case we have a two-parameter excitation:

$$\epsilon(\lambda_{1h}, \lambda_{2h}) = \epsilon(\lambda_{1h}) + \epsilon(\lambda_{1h}) \tag{43}$$
$$p(\lambda_{1h}, \lambda_{2h}) = p(\lambda_{1h}) + p(\lambda_{1h}) \qquad -\frac{\pi}{2} \leqslant \lambda_{1h}, \lambda_{2h} \leqslant \frac{\pi}{2}. \tag{44}$$

The triplet excitation spectra for various fillings in the hyperbolic region ($\Delta = \cosh\gamma$ with $\gamma = 2$) are shown in figure 5. We have here massive spin excitation modes with non-linear dispersion, whereas for the usual *t*–*J* model we have the massless excitation mode with quasi-linear dispersion [8]. At half-filling (i.e., for the *XXZ*-model), notably, we find a spin excitation mode lower than that obtained by des Cloizeaux and Gaudin [29]. They calculated the triplet excitations in the same spirit as des Cloizeaux and Pearson [30] who treated the spin-$\frac{1}{2}$ isotropic Heisenberg (XXX-) model. The des Cloizeaux–Gaudin mode is given by [28]

$$\epsilon(p) = \frac{2K}{\pi}\sinh\gamma\sqrt{1 - k^2\cos^2 p} \qquad 0 \leqslant p \leqslant 2\pi \tag{45}$$

which is obtained by eliminating λ_{1h} from (43) and (44) with λ_{2h} fixed at $\pm\pi/2$. As is explained by Faddeev and Takhtajan [27], this family of states is a special one-parameter subfamily of two-parameter states. It is true that the energy and the momentum of excitations are given additively by those of the individual holes with the dispersion of the same form as (45) but with $0 \leqslant p \leqslant \pi$. However, the energy $\epsilon(p)$ is an implicit function of the momentum and the lowest excitation mode is *not* necessarily given by (45) if the excitation has a non-linear dispersion. (The des Cloizeaux–Gaudin spectrum was previously criticized by Ishimura and Shiba [31] using the perturbation theory.) In the present case, the *true* lowest excitation mode near $p = 0$ (and 2π) is given by

$$\epsilon(p) = \frac{2K}{\pi}\sinh\gamma\left[2\sqrt{1-k^2\cos^2\frac{p}{2}} - \sqrt{1-k^2}\right] \qquad 0 \leqslant p \leqslant 2\pi \tag{46}$$

instead of (45) [32]. This form of the dispersion law is obtained by letting $\lambda_{1h} = \lambda_{2h} = \lambda_h$ and eliminating λ_h from (43) and (44). Note that (45) and (46) give the same result for the sound velocity. In the isotropic limit $\gamma \to 0$, equation (45) gives the des Cloizeaux–Pearson mode $\epsilon(p) = \pi|\sin p|$, while (46) gives the dispersion $\epsilon(p) = 2\pi\sin(p/2)$ that is the upper bound of the continuum of the triplet excitation of the spin-$\frac{1}{2}$ (isotropic) Heisenberg model.

Spin excitations of the second type are constructed by making a state with $2N-2$ holes and the only one 'string' of length n (an n-string [33, 34]):

$$\lambda_{n,j} = \lambda_s + \mathrm{i}\frac{\gamma}{2}(n+1-2j) \qquad j = 1, \ldots, n. \tag{47}$$

The centre λ_s of the string is not an independent parameter and is determined at arbitrary filling by the condition (neglecting the terms of order $1/L$)

$$L\theta_n(\lambda_s) = \sum_{j=1}^{M'}[\theta_{n-1}(2(\lambda_s - \lambda_{jh})) + \theta_{n+1}(2(\lambda_s - \lambda_{jh}))] + \sum_{\alpha=1}^{N_h^{(0)}}\theta_n(\Lambda_\alpha - \lambda_s) \tag{48}$$

where $M' = N_\downarrow^{(0)} + N_h^{(0)} - N$ (superscript '(0)' indicates the ground state) and $\theta_n(\alpha) = 2\arctan[\coth(\frac{1}{2}\gamma n)\tanh\alpha]$. For the excitation of the present type the Bethe *ansatz* equations in the thermodynamic limit take the form

$$\begin{aligned}\rho_s(\lambda) = S_2(\lambda) &+ \int_{-Q}^{Q}\mathrm{d}\lambda'\ S_1(\lambda-\lambda')\rho_s(\lambda) + \int_{-B}^{B}\mathrm{d}\Lambda'\ S_2(\lambda-\Lambda')\rho_c(\Lambda') \\ &- \frac{1}{L}\sum_{j=1}^{2N-2}\delta(\lambda-\lambda_{jh}) - \frac{1}{L}(T_{n-1}(\lambda-\lambda_s) + T_{n+1}(\lambda-\lambda_s)) \\ \rho_c(\Lambda) = \int_{-Q}^{Q}&\mathrm{d}\lambda'\ S_2(\Lambda-\lambda')\rho_s(\lambda') + \frac{1}{L}T_n(\lambda-\lambda_s)\end{aligned} \tag{49}$$

where the inhomogeneous term $T_n(\alpha)$ is given by

$$T_n(\alpha) = \frac{1}{\pi}\frac{\sinh n\gamma}{\cosh n\gamma - \cos(2\alpha)}. \tag{50}$$

Defining

$$\psi(\lambda,\Lambda) \equiv \begin{pmatrix}\psi_1(\lambda)\\ \psi_2(\Lambda)\end{pmatrix} = \begin{pmatrix}-\sum_{j=1}^{2N}\delta(\lambda-\lambda_{jh}) - T_{n-1}(\lambda-\lambda_s) + T_{n+1}(\lambda-\lambda_s)\\ T_n(\lambda-\lambda_s)\end{pmatrix} \tag{51}$$

we have a set of equations similar to (35). It then follows that the excitation energy is given by

$$\epsilon = \varepsilon_{0s}(\lambda_s) + \sum_{\alpha=1}^{2}\int_{-a_\alpha}^{a_\alpha}\mathrm{d}\mu_\alpha\ \varepsilon_\alpha(\mu_\alpha)\psi_\alpha = -\varepsilon_s(\lambda_s) - \sum_{j=1}^{2N-2}\varepsilon_1(\lambda_{jh}) \tag{52}$$

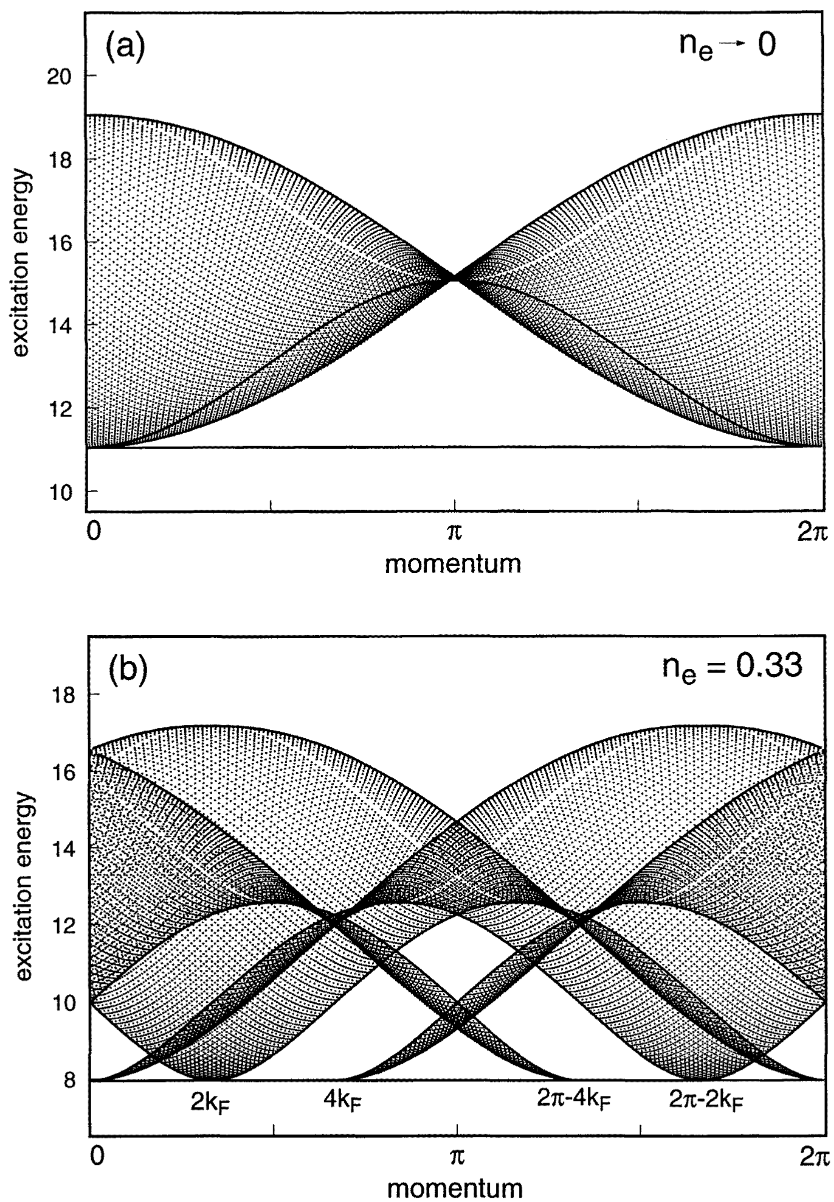

Figure 5. Spin excitations (triplet) for various electron densities n_e. The effective Fermi surface is at k_F. The anisotropy is $\Delta = \cosh\gamma$ with $\gamma = 2$. The continua are obtained by calculating the two-parameter excitations (43) and (44). The result for $n_e = 1$ gives the excitation spectrum of the spin-$\frac{1}{2}$ XXZ-chain. For $n_e \to 0$ the free-particle triplet excitation spectrum is reproduced.

where

$$\varepsilon_{0s}(\lambda_s) = -\frac{2\sinh^2 n\gamma}{\cosh n\gamma - \cos(2\lambda_s)} \tag{53}$$

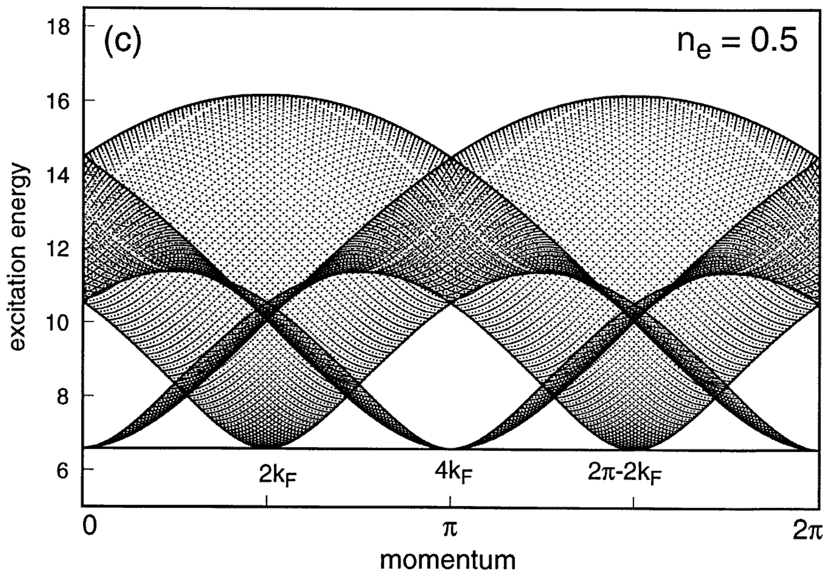

Figure 5. (Continued)

is the 'bare' energy of the n-string, and $\varepsilon_s(\lambda_s)$ denotes the dressed energy of the string which is defined by

$$\varepsilon_s(\alpha) = -\frac{2\sinh^2 n\gamma}{\cosh n\gamma - \cos(2\alpha)} - \int_{-Q}^{Q} \mathrm{d}\lambda' \, \frac{\mathrm{d}}{\mathrm{d}\lambda}[\theta_{n-1}(2(\lambda - \lambda')) + \theta_{n+1}(2(\lambda - \lambda'))]\varepsilon_1(\lambda') + \int_{-B}^{B} \mathrm{d}\Lambda \; T_n(\lambda - \Lambda)\varepsilon_2(\Lambda). \tag{54}$$

It is easy, using the integral equations for $\varepsilon_1(\lambda)$ and $\varepsilon_2(\Lambda)$, to show that $\varepsilon_s(\lambda_s) = 0$, i.e., the string has no contribution to the energy of excitation. Thus, the excitation energy is just the same as that of an excitation with $2N - 2$ holes only. Similarly, we can also show that we have the same expression for the momentum of excitation as (38) with N replaced by $N - 1$. The quantum numbers of the spin are found to be $S = S^z = N - n$. For $N = n = 2$ we have the spin-singlet excitation which has the same energy and momentum as those of the spin-triplet excitation of the first type considered above.

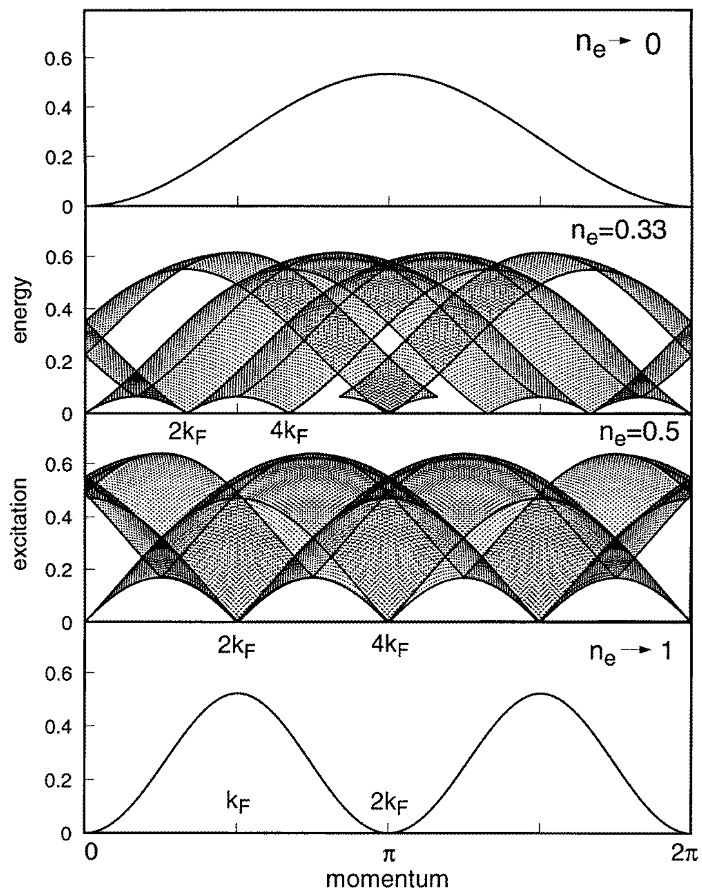

Figure 6. Charge excitations (particle–hole) for various electron densities n_e. The effective Fermi surface is at $2k_F$. The anisotropy is $\Delta = \cosh\gamma$ with $\gamma = 2$. The continua are obtained by calculating the two-parameter excitations (58) and (60), except for in the two limiting cases $n_e \to 0, 1$. In the low-density limit $n_e \to 0$, only the 'hole' part of the spectrum is present. For $n_e \to 1$, on the other hand, only the 'particle' part survives.

3.2. Charge excitations

Keeping the number of electrons fixed, we obtain the holon–antiholon (particle–hole) excitation which is constructed by varying the distribution of Λ, leaving the spin configuration unchanged. We make a 'hole' by removing one rapidity of Λ_h ($|\Lambda_h| \leqslant B$)

from the ground-state distribution and create a 'particle' Λ_p outside the Fermi boundary B. For those excitations in the thermodynamic limit we deal with the following set of coupled integral equations:

$$\rho_s(\lambda) = S_2(\lambda) + \int_{-Q}^{Q} d\lambda' \ S_1(\lambda - \lambda')\rho_s(\lambda) + \int_{-B}^{B} d\Lambda' \ S_2(\lambda - \Lambda')\rho_c(\Lambda) + \frac{1}{L} S_2(\lambda - \Lambda_p)$$
$$\rho_c(\Lambda) = \int_{-Q}^{Q} d\lambda' \ S_2(\Lambda - \lambda')\rho_s(\lambda') - \frac{1}{L}\delta(\Lambda - \Lambda_h) \tag{55}$$

with the requirement

$$\int_{-B}^{B} d\Lambda \ \rho_c(\Lambda) = \frac{N_h^{(0)} - 1}{L}. \tag{56}$$

The 'backflow' distribution $\sigma(\lambda, \Lambda)$ again obeys equation (35), but with

$$\psi(\lambda, \Lambda) \equiv \begin{pmatrix} \psi_1(\lambda) \\ \psi_2(\Lambda) \end{pmatrix} = \begin{pmatrix} S_2(\lambda - \Lambda_p) \\ -\delta(\Lambda - \Lambda_h) \end{pmatrix}. \tag{57}$$

Similarly to the spin excitations, we can express the charge excitation energy in terms of the dressed energies:

$$\epsilon = \sum_{\alpha=1}^{2} \int_{-a_\alpha}^{a_\alpha} d\mu_\alpha \ \varepsilon_{0\alpha}(\mu_\alpha)\sigma_\alpha(\mu_\alpha) + \mu = \sum_{\alpha=1}^{2} \int_{-a_\alpha}^{a_\alpha} d\mu_\alpha \ \varepsilon_\alpha(\mu_\alpha)\psi_\alpha + \mu$$
$$= -\varepsilon_2(\Lambda_h) + \varepsilon_2(\Lambda_p) \geqslant 0 \tag{58}$$

(equality holds for $\Lambda_h = \Lambda_p$). Clearly, the charge excitation is massless for any anisotropy. The momentum of the excited states is given by

$$p = -\frac{2\pi}{L} \sum_\alpha I_\alpha = \frac{2\pi}{L}(I_p - I_h) \qquad (\mathrm{mod}\ 2\pi) \tag{59}$$

which yields, in the thermodynamic limit,

$$p = 2\pi \int_{\Lambda_h}^{\Lambda_p} d\Lambda \ \rho_c^0(\Lambda) \qquad (\mathrm{mod}\ 2\pi). \tag{60}$$

As is the case for the isotropic case, we have additional branches at $\pm 2k_F$ ($k_F = \pi n_e/2$) [8]. Here again we have a two-parameter family of the excitation. The charge excitation spectrum for various fillings in the hyperbolic region ($\Delta = \cosh\gamma$ with $\gamma = 2$) is shown in figure 6. The effective charge Fermi surfaces are at $2k_F$. Note that the continuum of states disappears in the two limiting cases $n_e \to 0, 1$. In the low-density limit ($B = \frac{1}{2}\pi$, or $B \to \infty$), we can only create a 'particle' at the Fermi boundary $\pm B$ and the spectrum reduces to the one-parameter family of a hole. At half-filling $B = 0$, on the other hand, there is no room to make a 'hole' in the Λ distribution. Therefore, only the particle part survives ($|\Lambda_p| \leqslant \frac{1}{2}\pi$, or $|\Lambda_p| \leqslant \infty$).

4. Summary

We obtained the exact solution of the anisotropic supersymmetric t–J model in one dimension. We determined the ground-state properties in relation to the anisotropy. For $\Delta \geqslant 1$, the ground-state (at $h = 0$) and the magnetic properties are just those of the spin-$\frac{1}{2}$ XXZ-chain (the XXX-chain in the isotropic limit). For $\Delta < 1$, on the other hand, we found a continuous magnetic phase transition. The low-lying (spin and charge) excitation continuum is calculated for various electron fillings. We found that the charge excitations are massless for any value of the anisotropy. Whether the spin excitations are massive or massless depends on the anisotropy of the model. Remarkably, at half-filling (namely, for the spin-$\frac{1}{2}$ *XXZ*-model), we identified the correct lowest (spin) excitation mode which has previously not been known.

Acknowledgments

We would like to thank Y Akutsu for continuous encouragement and helpful suggestions. We are grateful to N Kawakami, V E Korepin and M Takahashi for valuable discussions and comments.

References

[1] Anderson P W 1987 *Science* **235** 1196
[2] Zhang F C and Rice T M 1988 *Phys. Rev.* B **37** 3759
[3] Anderson P W 1990 *Phys. Rev. Lett.* **64** 1839
[4] Lai C K 1974 *J. Math. Phys.* **15** 1675
[5] Sutherland B 1975 *Phys. Rev.* B **12** 3795
[6] Schlottmann P 1987 *Phys. Rev.* B **36** 5177
[7] Sarkar S 1990 *J. Phys. A: Math. Gen.* **23** L409; 1991 *J. Phys. A: Math. Gen.* **24** 1137
[8] Bares P A, Blatter G and Ogata M 1991 *Phys. Rev.* B **44** 130
[9] Kawakami N and Yang S-K 1990 *Phys. Rev. Lett.* **65** 2309; 1991 *J. Phys.: Condens. Matter* **3** 5983
[10] Essler F H and Korepin V E 1992 *Phys. Rev.* B **46** 9147
[11] Quaisser M, Schadschneider A and Zittartz J 1992 *J. Phys. A: Math. Gen.* **25** L1127
[12] Förster A and Karowski M 1993 *Nucl. Phys.* B **408** 512
[13] Bariev R Z 1994 *J. Phys. A: Math. Gen.* **27** 3381
[14] Bariev R Z 1994 *Phys. Rev.* B **49** 1474
[15] Fei S-M and Yue R-H 1994 *J. Phys. A: Math. Gen.* **27** 3715
[16] Bariev R Z, Klümper A, Schadschneider A and Zittartz J 1995 *Z. Phys.* B **96** 395
[17] Suzuki J 1992 *J. Phys. A: Math. Gen.* **25** 1769
[18] Ogata M, Luchini M U, Sorella S and Assaad F F 1991 *Phys. Rev. Lett.* **66** 2388
[19] Cherednik I V 1980 *Theor. Math. Phys.* **43** 356
[20] Perk J H H and Schultz C L 1981 *Phys. Lett.* **84A** 407
[21] Babelon O, de Vega H J and Viallet C M 1982 *Nucl. Phys.* B **200** 266
[22] Yang C N and Yang C P 1966 *Phys. Rev.* **150** 321, 327
[23] Izergin A G, Korepin V E and Reshetikhin N Yu 1989 *J. Phys. A: Math. Gen.* **22** 2615
[24] Woynarovich F 1989 *J. Phys. A: Math. Gen.* **22** 4243
[25] Woynarovich F and Penc K 1991 *Z. Phys.* B **85** 269
[26] Quaisser M, Schadschneider A and Zittartz J 1994 *Z. Phys.* B **95** 427
[27] Faddeev L and Takhtajan L 1981 *Phys. Lett.* **85A** 375
[28] Johnson J D and McCoy B M 1972 *Phys. Rev.* A **4** 1613
[29] des Cloizeaux J and Gaudin M 1966 *J. Math. Phys.* **7** 1384
[30] des Cloizeaux J and Pearson J J 1962 *Phys. Rev.* **128** 2131
[31] Ishimura N and Shiba H 1980 *Prog. Theor. Phys.* **63** 743
[32] We heard from M Takahashi that he has also noticed this fact. We thank him for useful comments on reference [29].
[33] Takahashi M 1971 *Prog. Theor. Phys.* **46** 401
Takahashi M and Suzuki M 1972 *Prog. Theor. Phys.* **48** 2187
[34] Gaudin M 1971 *Phys. Rev. Lett.* **26** 1301